Tidal variability in the Hong Kong region

Adam T. Devlin

Department of Geography and the Environment, Jiangxi Normal University.

Nanchang, Jiangxi, China

Institute of Space and Earth Information Science, The Chinese University of Hong Kong, Shatin, Hong Kong SAR, China

Shenzhen Research Institute, The Chinese University of Hong Kong, Shenzhen, Guangdong, China

Jiayi Pan*

Department of Geography and the Environment, Jiangxi Normal University.

Nanchang, Jiangxi, China

Institute of Space and Earth Information Science, The Chinese University of Hong Kong, Shatin, Hong Kong SAR, China

Shenzhen Research Institute, The Chinese University of Hong Kong, Shenzhen, Guangdong, China

Hui Lin

Department of Geography and the Environment, Jiangxi Normal University.

Nanchang, Jiangxi, China

Institute of Space and Earth Information Science, The Chinese University of Hong Kong, Shatin, Hong Kong SAR, China

* - Corresponding author

~~Second re-submission to *Ocean Science*~~

~~May 2019~~

Abstract

Mean sea level (MSL) is rising worldwide, and correlated changes in ocean tides are also occurring. This combination may influence future extreme sea levels, possibly increasing coastal inundation and nuisance flooding events in sensitive regions. Analyses of a set of tide gauges in Hong Kong reveal complex tidal behavior. Most prominent in the results are strong correlations of MSL variability to tidal variability over the 31-year period of 1986-2016; these tidal anomaly correlations (TACs) express the sensitivity of tidal amplitudes and phases (M_2, S_2, K_1, O_1) to MSL fluctuations and are widely observed across the Hong Kong region. At a few important harbor locations, time series of approximations of the parameter δ-HAT, computed from combinations of the major tidal constituents, are found to be highly sensitive to MSL variability which may further increase local flood levels under future MSL rise. Other open-water locations in Hong Kong only show TACs for some individual tidal constituents but not for combined tidal amplitudes, suggesting that the dynamics in enclosed harbor areas may be partially frequency-dependent and related to resonance or frictional changes. We also observe positive correlations of the fluctuations of diurnal (D_1) tides to semidiurnal (D_2) tides at most locations in the region which may lead to further amplified tidal ranges under MSL. ~~Overall, it~~It is ~~shown~~ demonstrated here that tidal changes in the Hong Kong coastal waters may be important in combination with MSL rise in impacting future total water levels.

1. Introduction

Ocean tides have long been thought of as a stationary process, as they are driven by the gravitational forcing of the Sun and Moon whose motions are complex but highly predictable (Cartwright and Tayler, 1971). Yet, long-term changes in the tides have been observed recently on regional (Ray, 2006; Jay et al., 2009; Zaron and Jay, 2014; Rasheed and Chua, 2014; Feng et al., 2015; Ross et al., 2017) and worldwide spatial scales (Woodworth, 2010; Müller, et al. 2011; Haigh et al., 2014; Mawdsley et al., 2015), concurrent with long-term global mean sea level (MSL) rise (Church and White, 2006; 2011). Since gravitational changes are not the reason, the tidal changes are likely related to terrestrial factors such as changes in water depth which can alter friction (Arbic et al, 2009), coastal morphology and resonance changes of harbor regions (Cartwright, 1972; Bowen and Gray, 1972; Amin, 1983; Vellinga et al., 2014; Jay et al., 2011; Chernetsky et al., 2010, Familkhalili & Talke, 2016), or stratification changes induced by increased upper-ocean warming (Domingues et al., 2008; Colosi and Munk, 2006; Müller, 2012; Müller et al., 2012), all of which are also related to sea level rise.

Tides can also exhibit short-term variability correlated to short-term fluctuations in MSL (Devlin et al., 2014; 2017a; 2017b). These variabilities may influence extreme water level events, such as storm surge or nuisance flooding (Sweet and Park, 2014; Cherqui et al., 2015; Moftakhari et al., 2015; 2017; Ray and Foster, 2016; Buchanan et al., 2017). Such short-term extreme events are obscured when only considering long-term linear trends. Any significant additional shorter-term positive correlation between tides and sea level fluctuations may amplify this variability and would imply that flood risk based only on the superposition of present-day tides and surge onto a higher baseline sea level will be inaccurate in many situations. The analysis of the correlations between tides and sea level at a local or regional scale can indicate locations where tidal evolution should be considered as a substantial complement to sea level rise. Moreover, since storm surge is a long wave, factors affecting tides can also alter storm surge (Familkhalil and Talke, 2016; Arns et al., 2017). Hong Kong is often subject to typhoons, with some recent storms yielding anomalously high storm surges, so this issue is of critical interest if all such factors are undergoing change.

Recent works surveyed tidal anomaly correlations (TACs) at multiple locations in the Pacific;~~,~~ a ~~metric that~~TAC quantifies the sensitivity of tides to short-term sea level fluctuations (Devlin et al., 2014; Devlin et al., 2017a); they found ~~, finding~~ that over 90% of tide gauges analyzed exhibited some measure of correlation in at least one tidal component. In a related work (Devlin et al., 2017b), the combined TACs of the four largest tidal components was calculated as a proxy for what can be described as changes in the highest astronomical tide (δ-HAT), with 35% of gauges surveyed exhibiting a sensitivity of δ-HATs to sea level fluctuations of at least ± 50 mm under a 1-m sea level change (~5%). A step-by-step description of the TAC and δ-HAT methods, including the details of the calculations of the regressions and statistics, can be found in the supplementary materials of Devlin et al. (2017a and 2017b), and in this paper we summarize the meaning and interpretations of the TACs and the δ-HATs in the Appendix.

A recent paper performed a similar analysis ~~approach~~ in the Atlantic Ocean, finding comparable results to the Pacific (Devlin et al., 2019). Comparing all worldwide locations found that the greatest (positive) δ-HAT response was seen in Hong Kong (+ 650 mm m^{-1}). A probability distribution function analysis revealed that an extreme sea level exceedance which includes tidal changes can be nearly double (+150 mm) that which only considers MSL exceedance alone (+78 mm) over the past 50 years (Devlin et al., 2017b). However, this approach did not consider water level extremes due to non-tidal or non-MSL factors, such as storm surge, which may further complicate extreme water levels. Yet, even without storm surge included, it was demonstrated that the non-stationarity of tides can be a significant contributor to total (non-storm) water levels in this region and warrants closer examination. Furthermore, tides and storm surge are both long-wave processes and may be sensitive to the same forcing factors, so the behavior of tides may be a possible instructor of the future behavior of storm surge events.

Hong Kong and the Pearl River Delta (PRD) region contains many densely-populated areas with extensive coastal infrastructure and significant and continuous recent land reclamation projects. Sea level rise in the region has exhibited a variable rate in the region over the past 50 years (Li and Mok, 2012; Ip and Wai, 1990), but a common feature of all sea level records in the South China Sea (SCS) is a steep increase in the late 1990s with a subsequent decrease in the early 2000s, followed by a sustained increase to the present day. In addition to this variable MSL behavior, there are also anomalous tidal events observed at gauges in semi-enclosed harbor regions during the late 1990s and early 2000s (shown and

discussed below), corresponding to times of both rapidly changing sea level and aggressive land reclamation. In this study, we perform a spatial and temporal analysis of tidal sensitivity to MSL variations in Hong Kong using the tidal anomaly correlation (TAC) method at 12 closely-located tide gauges.

2. Methods

2.1 Data sources

A set of 12 tide gauge records in the Hong Kong region were provided by the Hong Kong Observatory (HKO) and the Hong Kong Marine Department (HKMD), spanning from 12 to 63 years in length, including two gauges that are "historical" (i.e., no longer operational). The longest record is the North Point/Quarry Bay tide gauge, located in Victoria Harbor, established originally in 1952 and relocated from North Point to Quarry Bay in 1986. The datums were adjusted and quality controlled by HKO to provide a continuous record (Ip and Wai, 1990). Another long and continuous record is located at Tai Po Kau inside Tolo Harbor. Gauge locations in Hong Kong are shown in Figure 1, with the gauges from HKO indicated by green markers, gauges from HKMD by light blue, and historical (non-operational) gauges by red. Four of six of the HKO gauges (Quarry Bay, Tai Po Kau, Tsim Bei Tsui, and Waglan Island) are sea level pressure transducer types of gauges, and the other two (Shek Pik and Tai Miu Wan) are pneumatic type tide gauges. The Quarry Bay gauge was updated from a float type gauge recently (2017), and the Tai Po Kau gauge was also updated from a float gauge in 2006, and all gauges operated by the HK Marine Department were ~~all~~ set up in 2004 as sea level pressure transducers (*https://www.hko.gov.hk/publica/pubsmo.htm*).

Figure 2 shows the geographical setting of the South China Sea, with the location of Hong Kong indicated by the red box. Table 1 lists the metadata for all locations, including station name and station code, latitude .... and the ranges of the data records used in this study. *2.2 Tidal admittance calculations*

Our investigations of tidal behavior use a tidal admittance method. The tidal admittance is the unitless ratio of an observed tidal constituent to the corresponding tidal constituent in the astronomical tide generating force expressed as a potential, V. This potential can then be divided by the acceleration due to gravity, g, to yield $Z_{pot}(t) = V/g$, with units of length that can be compared to tidal elevations, $Z_{obs}(t)$.. Yearly harmonic analyses are performed on both $Z_{obs}(t)$ and $Z_{pot}(t)$ at each location, using the R_T_TIDE package for

MATLAB (Leffler and Jay, 2009), a robust analysis suite based on T_TIDE (Pawlowicz, 2002). The tidal potential is determined based on the methods of Cartwright and Tayler (1971).

The result from a single harmonic analysis of $Z_{obs}(t)$ or $Z_{pot}(t)$ determines an amplitude, A, and phase, θ, at the central time of the analysis window for each tidal constituent, with error estimates. A moving analysis window (e.g., at mid-year) produces an annual time-series of amplitude, $A(t)$, and phase, $\theta(t)$, with the complex amplitude, $\mathbf{Z}(t)$, given by:

$$\mathbf{Z}(t) = A(t)e^{i\theta(t)} \quad . \tag{1}$$

The tidal admittance (**A**) and phase lag (**P**) are formed using Eqs. (2) and (3)

$$\mathbf{A}(t) = abs\left|\frac{\mathbf{Z}_{obs}(t)}{\mathbf{Z}_{pot}(t)}\right| \quad , \tag{2}$$

$$\mathbf{P}(t) = \theta_{obs}(t) - \theta_{pot}(t) \quad . \tag{3}$$

Nodal variabilities are typically present with similar strengths in both the observed tidal record and in the tidal potential. Therefore, when the observed data (harmonically analyzed in one-year windows) is divided by the potential (also analyzed in one-year windows), nodal effects are mostly constrained in the resulting admittance time series. This may not always hold true in shallow-water areas (Amin, 1983) but does seem ~~to~~ valid for the locations and tides analyzed in Hong Kong. The harmonic analysis procedure also provides an annual MSL time-series. For each resultant dataset (MSL, **A** and **P**), the mean and trend are removed from the time series to allow direct comparison of their co-variability. The magnitude of the long-term trends is typically much less than the magnitude of the short-term variability, which is more apparent in the data sets used here (Devlin et al., 2017a; 2017b).

Tidal sensitivity to sea level fluctuations is quantified using tidal anomaly correlations (TACs), the relationships of detrended tidal variability to detrended MSL variability (see Appendix). With the use of the TACs we determine the sensitivity of the amplitude and phase of individual constituents (M_2, S_2, K_1, O_1) to sea level perturbations at the yearly-analyzed scale. We also consider a proxy for the change in the approximate highest astronomical tide (δ-HAT; see Appendix for details). The approximation ~~e~~ δ-HAT reflects the maximum tide-related water level that would be obtained in a year from a combination of time-dependent amplitudes and ~~phases of~~phases of the four largest tidal ~~amplitudes~~ constituents (M_2, S_2, K_1, and O_1) extracted by the admittance method, typically ~75% of the full tidal range..

The detrended time series of the year-to-year change of the δ-HATs are compared to detrended yearly MSL variability in an identical manner as the TACs, and both are expressed in units of millimeter change in tidal amplitude per 1-meter fluctuation in sea level (mm m^{-1}). These units are adopted for convenience, though in practice, the observed fluctuations in MSL are on the order of ~ 0.25 m. The phase TACs are reported in units of degree change per 1-meter fluctuation in sea level. The TAC methodology can also be used to examine correlations between different parts of the tidal spectrum. We additionally examine the sensitivity of combined diurnal (D_1; $K_1 + O_1$) tidal amplitudes to semidiurnal (D_2; $M_2 + S_2$) tidal amplitudes (D_1/D_2 TACs). The units of the D_1/D_2 TACs are dimensionless (i.e., mm/mm), and statistics are calculated as above.

The use of a window of a year in a harmonic analysis may have an influence on the value of the TAC or δ-HAT, e.g. calendar year (Jan-Dec) vs. water year (Oct-Sep). To provide a better estimate of the overall correlations for all data we take a set of determinations of the correlations using twelve distinct year definitions (i.e., one-year windows running from Jan-Dec, Feb-Jan, …, Dec-Jan.). We take the average of the set of significant determinations (i.e., *p*-values of < 0.05) as the magnitude of the TAC or δ-HAT. For an estimate of the confidence interval of the TAC or δ-HAT, the interquartile range (middle 50% of the set) is used.

For the very long record stations (e.g., Quarry Bay and Tai Po Kau), we only consider the past 31 years for TAC and δ-HAT determinations (Table 1). The TAC values may change over time, so we adopt a common epoch to better match the rest of the Hong Kong tide gauge networks, which are typically ~12-31 years long. Finally, we highlight some anomalous tidal events observed at certain Hong Kong gauges, and discuss the temporal evolution of the tidal characteristics in Hong Kong.

3. Results

The individual TACs for amplitude and phase in Hong Kong are discussed first, followed by the δ-HATs and the D_1/D_2 TACs. In all figures, significant positive results will be reported by red markers, significant negative results by blue markers, and insignificant values are shown as black markers. The relative size of the markers will indicate the relative magnitude of the TAC or δ-HAT according the legend scale on each plot. All numerical results for the major amplitude TACs (M_2, S_2, K_1, and O_1) are listed in Table 2, and the δ-

HATs and D_1/D_2 TACs are listed in Table 3. Phase TACs of the individual constituents are reported in Table S1 of the supplement.

3.1 Tidal anomaly correlations (TACs)

The strongest positive M_2 TACs are seen at Quarry Bay (+218 ± 37 mm m^{-1}), and at Tai Po Kau (+267 ± 42 mm m^{-1}), with a smaller positive TAC seen at Shek Pik (Figure 3). In the waters west of Victoria Harbour, all other gauges except Kwai Chung exhibit moderate negative TACs. The semidiurnal phase TACs in Hong Kong (shown in the Supplementary materials, Figure S1) show an earlier M_2 tide under higher MSL at Quarry Bay and Tai Po Kau and a later tide west of Victoria Harbour. The S_2 results in Hong Kong (Figure 4) show that only Quarry Bay and Tai Po Kau have significant amplitude TAC values (though smaller than M_2), and the S_2 phase TACs in Hong Kong (Figure S2) also show an earlier tide at Quarry Bay and Tai Po Kau under higher MSL.

The diurnal TACs in Hong Kong generally exhibit a larger-magnitude and more spatially-coherent response than semidiurnal TACs. Like M_2, the strongest K_1 values in Hong Kong (Fig 5) are seen at Quarry Bay (+220 ± 15 mm m^{-1}) and Tai Po Kau (+190 ± 68 mm m^{-1}). The O_1 results in Hong Kong (Fig 6) are like the M_2 results, showing positive TACs at Quarry Bay (+146 ± 11 mm m^{-1}) and Tai Po Kau (+100 ± 25 mm m^{-1}), and strongly negative TACs west of Quarry Bay. However, unlike the semidiurnal constituents, the phase TACs for K_1 are mostly insignificant in Hong Kong (Figure S3), and O_1 phase TACs (Figure S4) are only significant at Quarry Bay.

3.2 Combined tidal variability (δ-HATs) and tidal co-variability

The TACs are widely observed in Hong Kong, but the δ-HATs are only of significance at particular locations (Figure 7). Five stations exhibit significant δ-HAT values, with Quarry Bay and Tai Po Kau having very large positive magnitudes (+665 ± 85 mm m^{-1} and +612 ± 210 mm m^{-1}, respectively), and Shek Pik having a lesser magnitude of +138 ± 47 mm m^{-1}. Conversely, Ma Wan and Chi Ma Wan exhibit moderate negative δ-HAT values, (~ -100 mm m^{-1}). The remainder of gauges (which are mainly open-water locations) have statistically insignificant results for the combined tidal amplitudes, even where some large individual TACs were observed. This shows that the combined tidal amplitude effect as expressed by the δ-HATs is most important in semi-enclosed harbors. The D_1/D_2 TACs are also important in Hong Kong and are seen at almost every location. All significant D_1/D_2 TACs results are positive (Figure 8), and at most locations the correspondence is nearly 1-to-

1, indicating that a change in D_1 can yield a nearly-identical magnitude change in D_2, and vice-versa. Smaller magnitude relations are seen in the western areas of the Hong Kong region.

3.3 Anomalous tidal events at Hong Kong harbor locations

The overall temporal behavior of the tidal spectrum at enclosed harbor locations in Hong Kong (Quarry Bay and Tai Po Kau) is especially interesting. In Figure 9, the time series of water level spectrum components are shown for Quarry Bay and Tai Po Kau, presenting the D_1 ($K_1 + O_1$) band (a), the D_2 ($M_2 + S_2$) band (b), and mean sea level (MSL) (c), given as normalized amplitudes with mean values shown in the legends. The magnitude of MSL is given in relation to the Hong Kong Chart Datum as defined by the Hong Kong Observatory. The Chart Datum is defined as 0.146 m below the Hong Kong Principal Datum (HKPD). The HKPD determined for the years 1965-1983 was approximately 1.23 m below MSL. The HKPD has been recently re-determined using data from 1997-2015 to be 1.30 m below MSL. Therefore, all MSL values reported here are given relative to the HKPD for the epoch 1965-1985. (www.hko.gov.hk).

Some very notable features of the tides are clear. At Quarry Bay, the early part of the record shows nearly constant tidal amplitudes in D_1, while D_2 amplitudes show a slight decrease, and MSL exhibits a slight positive trend. In the late 1980s, however, both D_1 and D_2 increase until around the year 2003, at which time both tidal bands undergo a rapid decrease of amplitude of ~15%, sustaining this diminished magnitude for about five years before increasing nearly as rapidly. ~~The OT band shows a sustained increase over the historical record, but many of the fluctuations around the trend are negatively correlated with the perturbations in D_1 and D_2, and during the times of diminished major tides, the OTs increase by about +20%.~~ The MSL record is also highly variable at Quarry Bay, with a nearly zero trend during the increase in tides seen in the 1980s, followed by a strong increase from ~1993-2000, and then a steep decrease concurrent with the time of diminished tides before increasing again. The gauge at Tai Po Kau shows a similar tidal behavior, although the timing and magnitudes are different. The increase in D_1 and D_2 at Tai Po Kau in the 1980s is much larger and peaks earlier than Quarry Bay, reaching a maximum around 1996, and then decreasing around 1998, about five years before the drop at Quarry Bay. Both locations experience an absolute minimum around 2007 in D_2, but the D_1 minimum at TPK

leads the Quarry Bay minimum by a few years. These observed anomalies are only observed at these two gauges; other locations in Hong Kong did not reveal similar behavior.

4. Discussion

4.1 Summary of observed tidal variability

This survey has identified several types of tidal variability in Hong Kong. The individual TACs are significant at many Hong Kong locations, while the TACs of the approximate δ-HATs appear to be more locally important, as the strongest responses are mainly concentrated at specific locations (e.g., Quarry Bay and Tai Po Kau). The M_2 response (Fig 3) is negative at gauges just west of Quarry Bay and positive at Shek Pik, with a similar pattern seen for the O_1 TACs (Fig 6). Conversely, the K_1 TAC results are generally positive (Fig 5). At both Quarry Bay and Tai Po Kau, the positive reinforcements of individual tidal fluctuations lead to very large δ-HATs, though moderately negative δ-HATs are seen near Quarry Bay at Chi Ma Wan and Ma Wan (Fig 7). The spatial similarity in the semi-enclosed center harbor regions suggest a connected mechanism; this area is where most recent Hong Kong coastal reclamation projects have occurred, including the construction of a new island for an airport, shipping channel deepening and other coastal morphology changes. Such changes in water depth and coastal geometry strongly suggest a relation to frictional or resonance mechanisms.

The D_1/D_2 TAC relations (Fig 8) are a more regionally-relevant phenomenon, being significant nearly everywhere in Hong Kong. The majority of significant D_1/D_2 TACs are positive, with most being nearly 1-to-1 (i.e., a ~1-mm change in D_1 will yield a ~1-mm change in D_2), confirmed by the close similarity of temporal tidal trends of the D_1 and D_2 tidal bands in Hong Kong (Fig 9). This aspect of tidal variability in Hong Kong may be related to the dynamics near the Luzon Strait, where large amounts of baroclinic conversion in both D_1 and D_2 tides may tend to couple the variabilities (Jan et al., 2007; 2008; Lien et al., 2015; Xie et al., 2008; 2011; 2013). The D_1 and D_2 internal tides may interact with each other as well as with processes at other frequencies, such as at the local inertial frequency, *f*, via parametric subharmonic instability (PSI) interactions (McComas and Bretherton, 1977; MacKinnon and Winters, 2005; Alford, 2008; Chinn et al., 2012), a form of resonant triad interactions (Craik, 1985). The low-mode baroclinic energy can travel great distances, being enhanced upon arrival at the shelf and leading to the further generation of baroclinic energy. In the western part of Hong Kong, the D_1/D_2 relationships are less than 1 to 1 (~0.33 to ~0.25

at TBT and LOP, respectively). This may be partially influenced by effects of the Pearl River, which discharges part of its flow along the Lantau Channel. The flow of the river is highly seasonal and ejects a freshwater plume at every ebb tide that varies with prevailing wind conditions and with the spring-neap cycle (Pan et al, 2014). The plumes may affect turbulence and mixing in the region and can dissipate tidal energy , which may "decouple" the correlated response of D_1 and D_2 seen in the rest of the Hong Kong coastal waters.

4.2 Effects of local dynamics on tidal variability

Hong Kong has had a long history of land reclamation to accommodate an ever-growing infrastructure and population, including the building of a new airport island (Chep Lap Kok), new land connections, channel deepening to accommodate container terminals, and many bridges, tunnels, and "new cities", built on reclaimed land. All of these may have changed the resonance and/or frictional properties of the region. Tai Po Kau has also had some land reclamation projects that have changed the coastal morphology and may have modulated the tidal response. Both locations also show coherent D_1/D_2 TACs, as well as having the largest positive δ-HATs, and large tidal anomalies (Figure 9). Other locations in Hong Kong did not show such extreme variations, so these variations appear to only be amplified in harbor areas. Decreases in friction associated with sea level rise may lead to ~~higher forcing of th~~larger~~e~~ tides, and those changes may also be amplified by the close correlations of D_1 and D_2 variability or local harbor development which may further decrease local friction. Hence, a small change in friction due to a small sea level change may induce a significant change in tidal ~~amplitudes~~constituents. The positive reinforcement of multiple tidal constituent correlated with regional sea level adjustments may amplify the risks of coastal inundation and coastal flooding, as evidenced by the gauges that had the largest δ-HAT values.

4.3 Limitations of this study and future steps

The analysis of tides in the Hong Kong tide gauge network revealed new dynamics and spatial connections in the area. However, some records are of shorter length and/or have many gaps, making a full analysis of the area problematic. For example, the Tsim Bei Tsui gauge covers a long period, but there are significant gaps in the record, which complicated our analysis. This gauge is located within a harbor region (Deep Bay), bordered to the north by Shenzhen, PRC, which has also grown and developed its coastal infrastructure in past decades, therefore, one might expect similar dynamics as was seen at Quarry Bay and Tai Po

Kau. While there were moderately significant D_1/D_2 correlations at Tsim Bei Tsui, no significant TACs or δ-HATs were observed. The large anomalies seen at Quarry Bay and Tai Po Kau around 2000 are suggested by the data at Tsim Bei Tsui, but some data is missing around this time, making any conclusions speculative. The Deep Bay region is ecologically sensitive, being populated by extensive mangrove forests which may be disturbed by rapidly changing sea levels (Zhang et al., 2018), so accurate determination of future sea levels is of utmost importance to the vitality of these important ecosystems. Future studies considering highly-accurate digital elevation models will employ simple analytical models as well as high resolution three-dimensional numerical ocean models to simulate the changing impacts on coastlines under a variety of sea level, tidal forcing, and anthropogenic change scenarios (historical and future), to better understand the tidal dynamics in Hong Kong, and to try to separate the relative importance of local and regional effects. Lastly, we ~~quickly~~ briefly mention the instrumental changes at two of the HKO gauges. The Quarry Bay gauge was updated from a float type gauge recently (2017), and the Tai Po Kau gauge was also updated from a float gauge in 2006. Neither of these times correspond to any obvious anomalies in the tidal admittance records (the large changes at Tai Po Kau predate this by a few years at least, and are consistent before and after the gauge change), so we conclude that the instrumental changes were not a factor in the observed variability.

5. Conclusions

This study has presented new information about the tidal variability in Hong Kong, based on observations of a set of closely-located tide gauges in Hong Kong. The TACs, D_1/D_2 relations, δ-HATs, and the anomalous events in tidal amplitudes seen at the Quarry Bay and Tai Po Kau gauges show an amplified tidal response to MSL fluctuations in these harbor regions as opposed to more open-water locations, where individual TAC were sometimes significant, but the ~~not as much for the~~ δ-HAT changes were less significant~~s~~. The reason for the observed behavior may be due to changing friction or resonance induced by coastal engineering projects that are only significant at highly local (i.e., individual harbor) scales. Alternatively, the observed behavior could be related to regional South China Sea changes due to climate change (such as increased upper-ocean warming and/or regional stratification and internal tide generation) ~~may also be a factor~~. It is difficult to separate the local engineering changes from regional climatic changes without closer investigations. However, even without exact knowledge of the relevant mechanisms, these anomalies do suggest that a pronounced change in tidal properties occurred around the year 2000 in Hong

Kong, with the effect being most pronounced at gauges in semi-enclosed harbors. Overall, the tidal variability in Hong Kong documented here may have significant impacts on the future of extreme sea level in the region, especially if the strong positive reinforcements hold or increase in coming decades. Short-term inundation events, such as nuisance flooding, may be amplified under scenarios of higher sea levels that lead to corresponding changes in the tides, which may amplify small changes in water levels and/or reductions in friction due to harbor improvements. The δ-HATs and D_1/D_2 TACs results illustrate that the tidal variability of multiple constituents may be additive, and may reinforce MSL changes at some locations, which may further aggravate coastal flooding under MSL future rise. Since tides and storm surge are both long-wave processes, the locations of strong tidal response may also experience an exaggerated storm surge in the near future.

Code availability All code employed in this study was developed using MATLAB, version R2011B. All code and methods can be provided upon request.

Data Availability The data used in this study from the Hong Kong Observatory (HKO; http://www.hko.gov.hk) and the Hong Kong Marine Department (HKMD; http://www.mardep.gov.hk/en/home.html) was provided upon request, discussion of intentions of use, and permission from the appropriate agency supervisors. Data used from the University of Hawaii Sea Level Center (UHSLC; http://www.uhslc.soest.hawaii.edu) is publicly available.

Appendix

A1. Tidal Anomaly Correlations (TACs)

Tidal admittances are constructed as described above, employing the use of the tidal potential and Equs. (2) and (3) to constrain the nodal variation present in the observed tidal amplitudes and phases. Our primary interest in this paper is the interannual to decadal variations and not the long-term trends in mean values. Therefore, we first remove the long-term trends and mean values using the MATLAB "detrend" function. The detrended time-series of residual variations in **A** and **P**, and the residual variations in MSL, can now be examined for coherence, using scatter plots, cross-correlations, and regression statistics. We define the tidal anomaly correlation (TAC) as the slope between detrended tidal properties

(amplitude and phase) and detrended MSL, expressed as the millimeter change in tidal amplitude per meter of sea level rise (mm m^{-1}). The same approach is used with the phase difference time-series to provide phase anomaly trends, with the trends expressed as degree change in tidal phase per meter of sea level rise (deg m^{-1}). The errors of the TAC determinations are defined as the 95% confidence interval (CI) of the linear trend determination. Trends are deemed significant if the signal-to-noise ratio (SNR) of the linear trend to the associated error is greater than 2.0.

A2. Approximate change in the highest astronomical tide (δ-HAT)

We also construct a "proxy" quantity as an approximate change in the highest astronomical tide (δ-HAT) using an extension of the TAC method. To do this, we combine the tidal admittance amplitudes of the (typically) four largest astronomical tides (M_2, S_2, K_1, and O_1), then detrend the resultant combined time series as above. Next, we perform a similar scatterplot and regression approach against the detrended MSL time series as was done with the TACs. The benefit of this approach is to give a clear picture of the overall changes in tides related to sea level changes. Some locations may show that the variability in multiple tidal constituents partially "cancel" each other (e.g., semidiurnal tides may have a large positive tendency compared to MSL variability while diurnal tides may have a large negative tendency, resulting in an offsetting of variabilities under MSL changes, and a smaller overall magnitude δ-HAT), while other locations may show a "reinforced" variability (e.g., both diurnal and semidiurnal tides have positive tendencies compared to MSL changes, resulting in an amplified δ-HAT). Thus, the accurate interpretation of the δ-HAT is that it reflects the maximum tide-related water level that would be obtained in a given analysis period (here, one year) from a chosen set of time-dependent amplitudes extracted from the admittance method.

Two details about the δ-HAT parameter should be noted here. First, only the amplitude of the tidal admittance can be combined in this manner, as combining the phase variability of multiple frequencies may be inaccurate at worst, and at best is not very helpful. Second, we acknowledge that the use of the term "δ-HAT" may be somewhat confusing, as previous literature about tidal analysis uses the term "Highest Astronomical Tide" (HAT) to denote the highest water level that can be expected to occur under average meteorological conditions due purely to astronomical forcing in a given epoch. This typical period is 19 years, which considers the full nodal cycle. This definition of HAT does not reflect the

highest *possible* water level at a given location, since storm surge or other "non-average" meteorological conditions may amplify water levels far above this level on a shorter time scale than a 19-year determination can reveal. The intention behind our chosen nomenclature of the "approximate change in the highest astronomical tide" (δ-HAT) attempts to expand on this concept by considering the "full" tidal variability (not strictly true since the 4 largest tides are only about 75% of the full tidal range, but these tidal components are nearly always stable in one year analyses, so it is a dependable and easily comparable metric) at timescales shorter than a nodal period (~19 years), but longer than a storm surge (~2-5 days) or other meteorological anomalies. Furthermore, our interest is the changes in tidal components that is not due to astronomy or to meteorology. Rather, we show possible changes to tide-related water level modifications due to MSL modifications, which may be important on seasonal to decadal time scales, induced by mechanisms associated with global climate change (e.g., steric sea level rise due to ice melt, thermal sea level rise due to upper-ocean warming), or to more local effects (such as rapid harbor modifications or land reclamation that adjusts tidal resonance at a particular location).

The changes shown by the δ-HATs are important to consider, since a full understanding of the changes in all components and timescales of the tides may better instruct future coastal planning and engineering. The δ-HAT method used here can give important information about possible future water level inundation in coastal locations that are not storm-related, such as nuisance flooding (or, sometimes called "sunny day flooding"). These may be obscured by longer-term analyses of the classical HAT (i.e., 19 years) if changes are more rapid (i.e., year-to-year or season-to-season). However, it should also be reiterated that a good understanding of changes in tides due to changing background water levels may also be instructive about future storm surge related inundation at a location; both tides and storms are long wave processes, so changes in one aspect of water level variability (i.e., a large positive δ-HAT) may also indicate future increase in storm surge levels at the same location.

Author Contributions ATD did all analyses, figures, tables, the majority of writing, and complied the manuscript. JP provided editing, insight, guidance, and direction to this study. HL provided critical insight and helpful input.

Competing Interests The authors declare they have no competing interests.

Acknowledgements This work is supported by The National Basic Research Program of China (2015CB954103), the National Natural Science Foundation of China (project 41376035), the General Research Fund of Hong Kong Research Grants Council (RGC) (CUHK 14303818), and the talent startup fund of Jiangxi Normal University. The authors also thank the Hong Kong Observatory. In addition to sharing their data archive, they were also a part of the discussions that led to this paper.

FIGURE CAPTIONS:

Figure 1 Tide gauge locations in Hong Kong used in this study. Green markers indicate active gauges provided by the Hong Kong Observatory (HKO), light blue markers indicate gauges provided by the Hong Kong Marine Department (HKMD), and red markers indicate historical gauges (once maintained by HKO) that are no longer operational.

Figure 2 Location of Hong Kong in the South China Sea, given by the red box, with some major oceanographic features labelled. Depth is given by the color bar, in units of meters.

Figure 3 Tidal anomaly correlations (TACs) of detrended M_2 amplitude to detrended MSL in Hong Kong, with the marker size showing the relative magnitude according to the legend, in units of mm m^{-1}. Red/blue markers indicate positive/negative TACs, and black markers indicate TACs which are not significantly different from zero.

Figure 4 Tidal anomaly correlations (TACs) of detrended S_2 amplitude to detrended MSL in Hong Kong, with the marker size showing the relative magnitude according to the legend, in units of mm m^{-1}. Red/blue markers indicate positive/negative TACs, and black markers indicate TACs which are not significantly different from zero.

Figure 5 Tidal anomaly correlations (TACs) of detrended K_1 amplitude to detrended MSL in Hong Kong, with the marker size showing the relative magnitude according to the legend, in units of mm m^{-1}. Red/blue markers indicate positive/negative TACs, and black markers indicate TACs which are not significantly different from zero. .

Figure 6 Tidal anomaly correlations (TACs) of detrended O_1 amplitude to detrended MSL in Hong Kong, with the marker size showing the relative magnitude according to the legend, in units of mm m^{-1}. Red/blue markers indicate positive/negative TACs, and black markers indicate TACs which are not significantly different from zero.

Figure 7 The tidal anomaly correlation computed from the combination of the four largest tidal constituent amplitudes (given by the detrended sum of the $M_2 + S_2 + K_1 + O_{1)}$ as a proxy for the change in the approximate highest astronomical tide (δ-HAT) relative to detrended MSL in Hong Kong, with the marker size showing the relative magnitude according to the legend, in units of mm m^{-1}. Red/blue markers indicate positive/negative TACs, and black markers indicate TACs which are not significantly different from zero.

Figure 8 The OT TACs; the relations of detrended diurnal tidal amplitude sum (D_1; $K_1 + O_1$) to detrended semidiurnal tidal amplitude sum (D_2; $M_2 + S_2$) in Hong Kong, with the marker size showing the relative magnitude according to the legend, in dimensionless units. Red/blue markers indicate positive/negative TACs, and black markers indicate TACs which are not significantly different from zero.

Figure 9 Time series of water level spectrum components at the Quarry Bay (QB; blue) and Tai Po Kau (TPK; red) tide gauges in Hong Kong, showing the D_1 band (a), the D_2 band (b), the OT band (c) and mean sea level (MSL) (d). Components are plotted as a function of normalized amplitudes to show relative variability, with mean values given in the legend.

FIGURES:

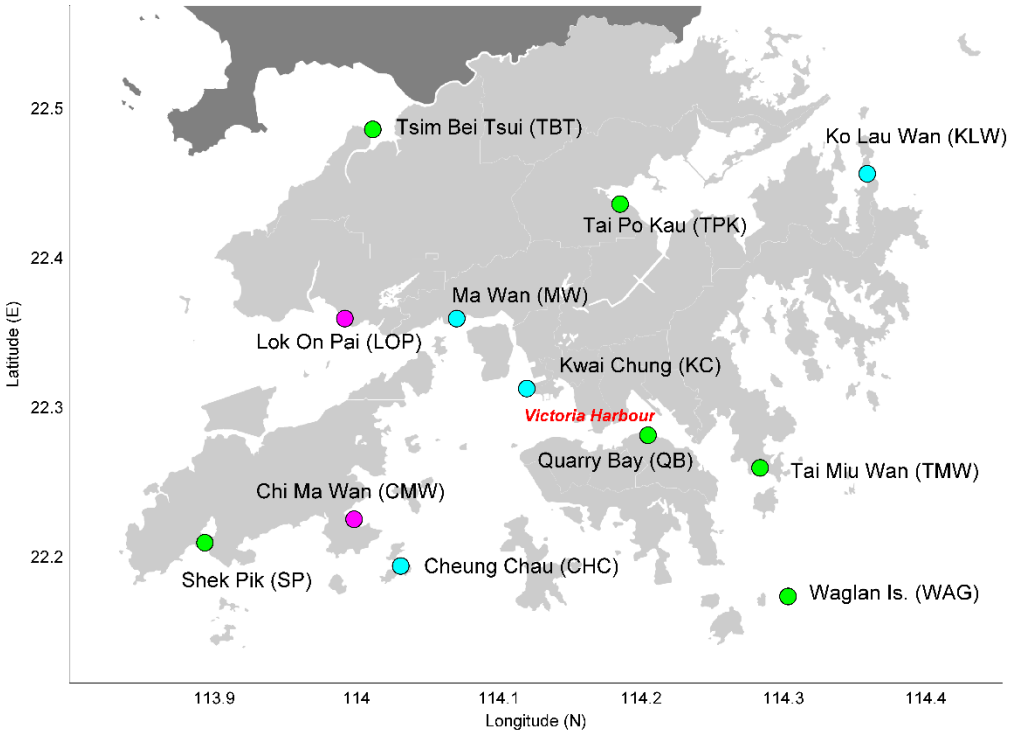

Figure 1 Tide gauge locations in Hong Kong used in this study. Green markers indicate active gauges provided by the Hong Kong Observatory (HKO), light blue markers indicate

gauges provided by the Hong Kong Marine Department (HKMD), and red markers indicate historical gauges (once maintained by HKO) that are no longer operational.

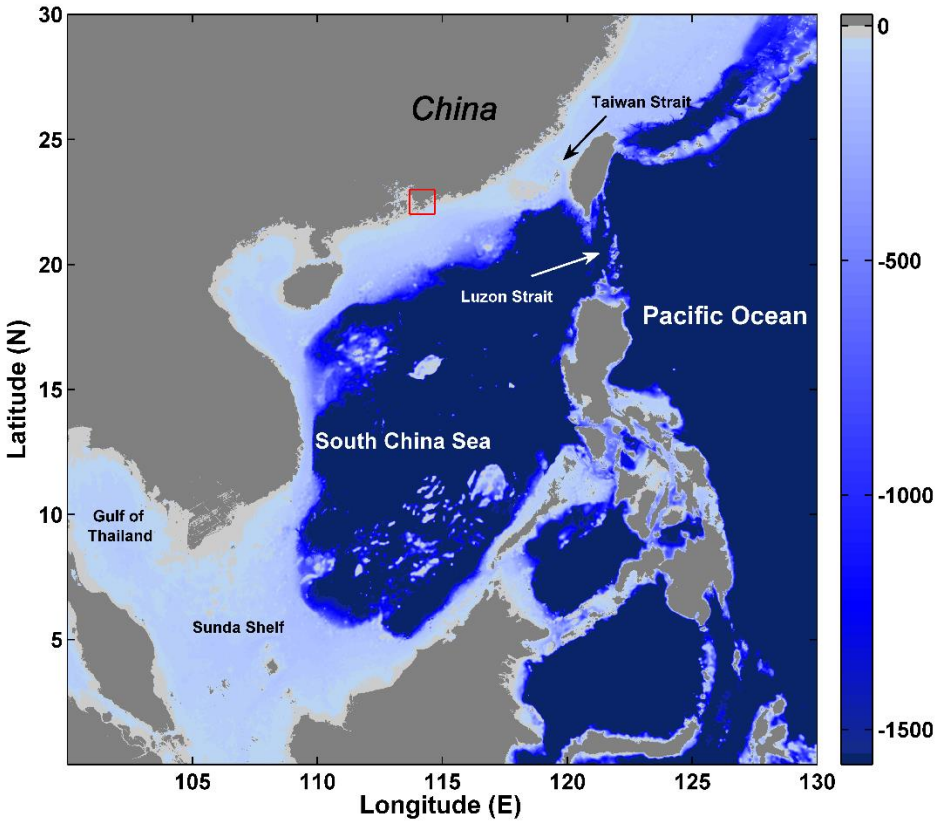

Figure 2 Location of Hong Kong in the South China Sea, given by the red box, with some major oceanographic features labelled. Depth is given by the color bar, in units of meters.

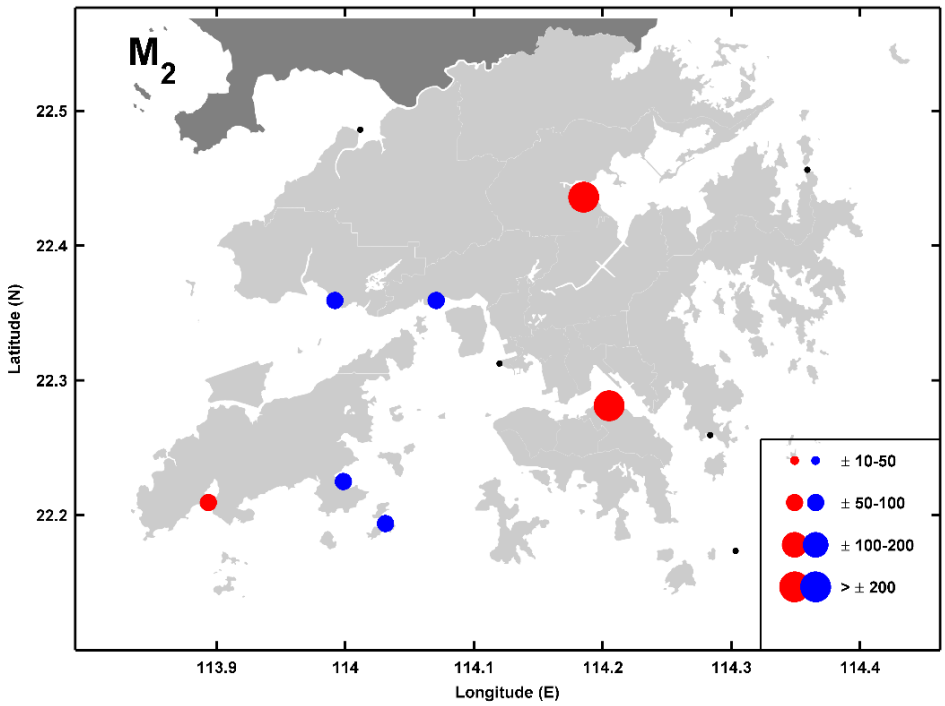

534

535 **Figure 3** Tidal anomaly correlations (TACs) of detrended M_2 amplitude to detrended MSL in
536 Hong Kong, with the marker size showing the relative magnitude according to the legend, in
537 units of mm m^{-1}. Red/blue markers indicate positive/negative TACs, and black markers
538 indicate TACs which are not significantly different from zero.

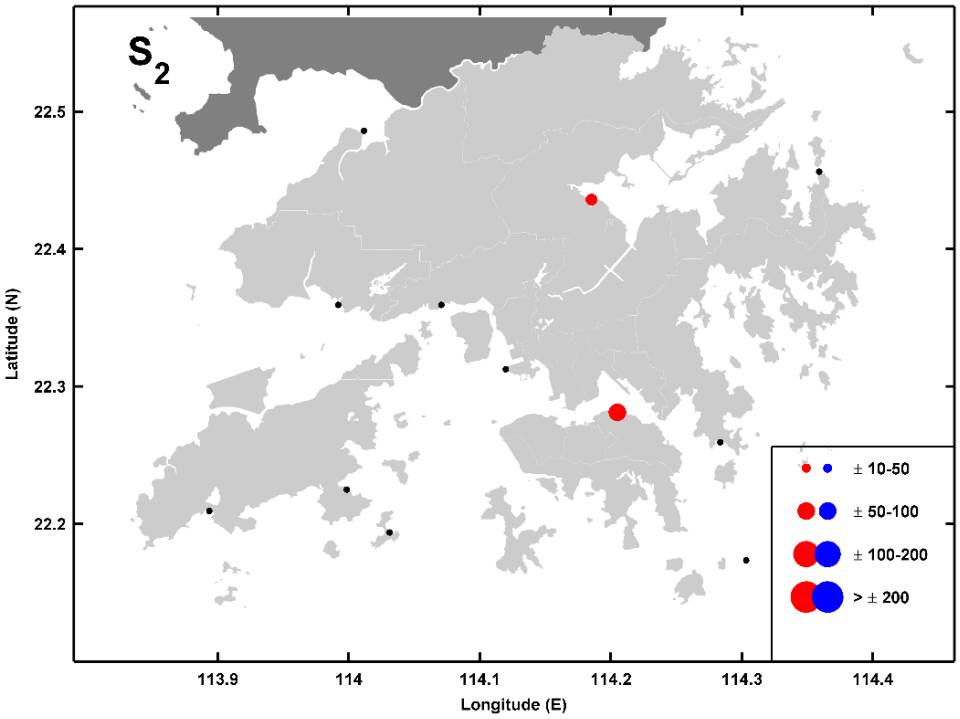

539

540 **Figure 4** Tidal anomaly correlations (TACs) of detrended S_2 amplitude to detrended MSL in
541 Hong Kong, with the marker size showing the relative magnitude according to the legend, in

542 units of mm m^{-1}. Red/blue markers indicate positive/negative TACs, and black markers
543 indicate TACs which are not significantly different from zero.

544

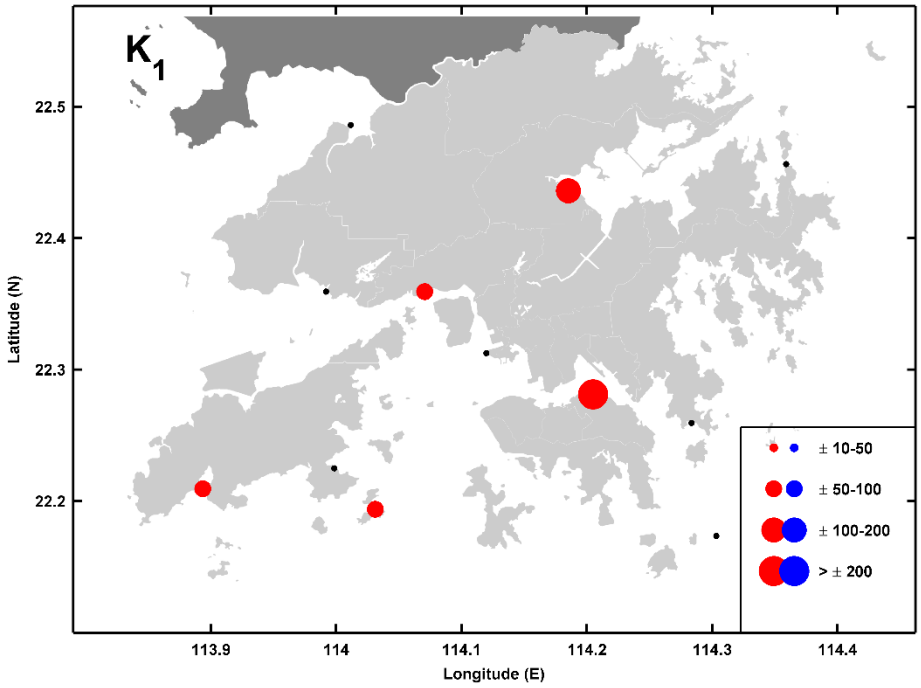

545

546 **Figure 5** Tidal anomaly correlations (TACs) of detrended K_1 amplitude to detrended MSL in
547 Hong Kong, with the marker size showing the relative magnitude according to the legend, in
548 units of mm m^{-1}. Red/blue markers indicate positive/negative TACs, and black markers
549 indicate TACs which are not significantly different from zero.

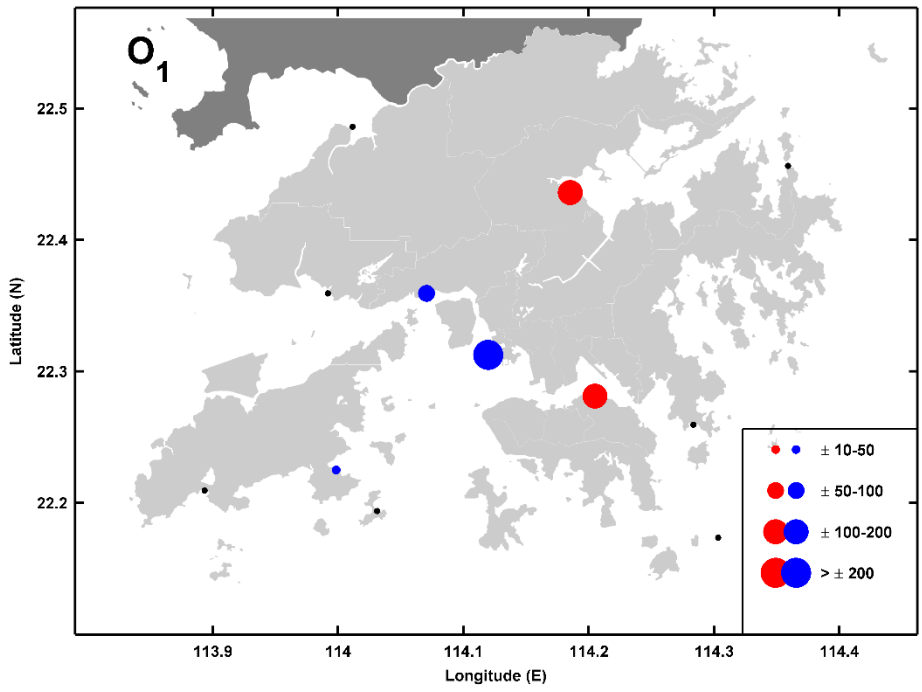

550

Figure 6 Tidal anomaly correlations (TACs) of detrended O_1 amplitude to detrended MSL in Hong Kong, with the marker size showing the relative magnitude according to the legend, in units of mm m^{-1}. Red/blue markers indicate positive/negative TACs, and black markers indicate TACs which are not significantly different from zero.

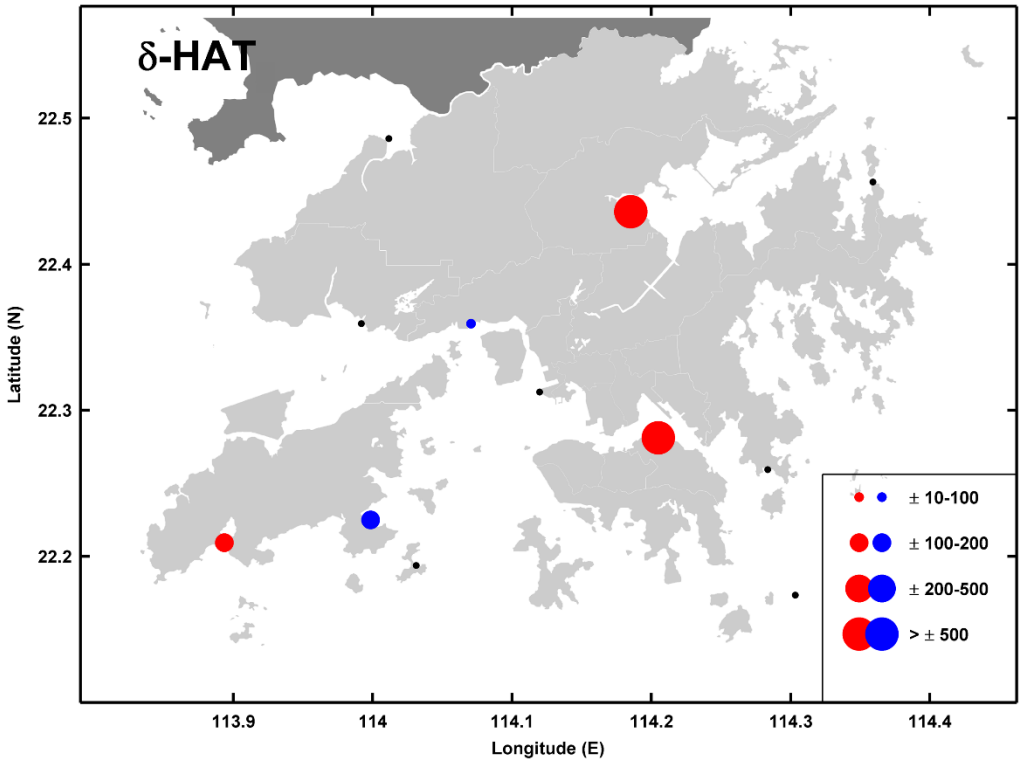

Figure 7 The tidal anomaly correlation computed from the combination of the four largest tidal constituent amplitudes (given by the detrended sum of the $M_2 + S_2 + K_1 + O_{1)}$ as a proxy for the change in the approximate highest astronomical tide (δ-HAT) relative to detrended MSL in Hong Kong, with the marker size showing the relative magnitude according to the legend, in units of mm m^{-1}. Red/blue markers indicate positive/negative TACs, and black markers indicate TACs which are not significantly different from zero.

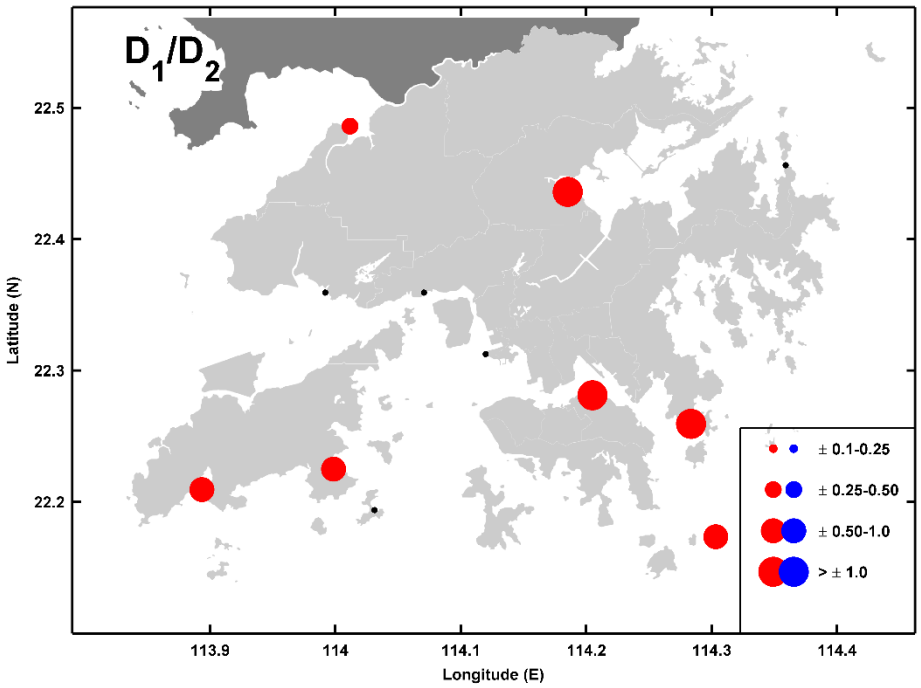

563

564 **Figure 8** The D_1/D_2 TACs; the relations of detrended diurnal tidal amplitude sum (D_1; K_1 +
565 O_1) to detrended semidiurnal tidal amplitude sum (D_2; M_2 + S_2) in Hong Kong, with the
566 marker size showing the relative magnitude according to the legend, in dimensionless units.
567 Red/blue markers indicate positive/negative TACs, and black markers indicate TACs which
568 are not significantly different from zero.

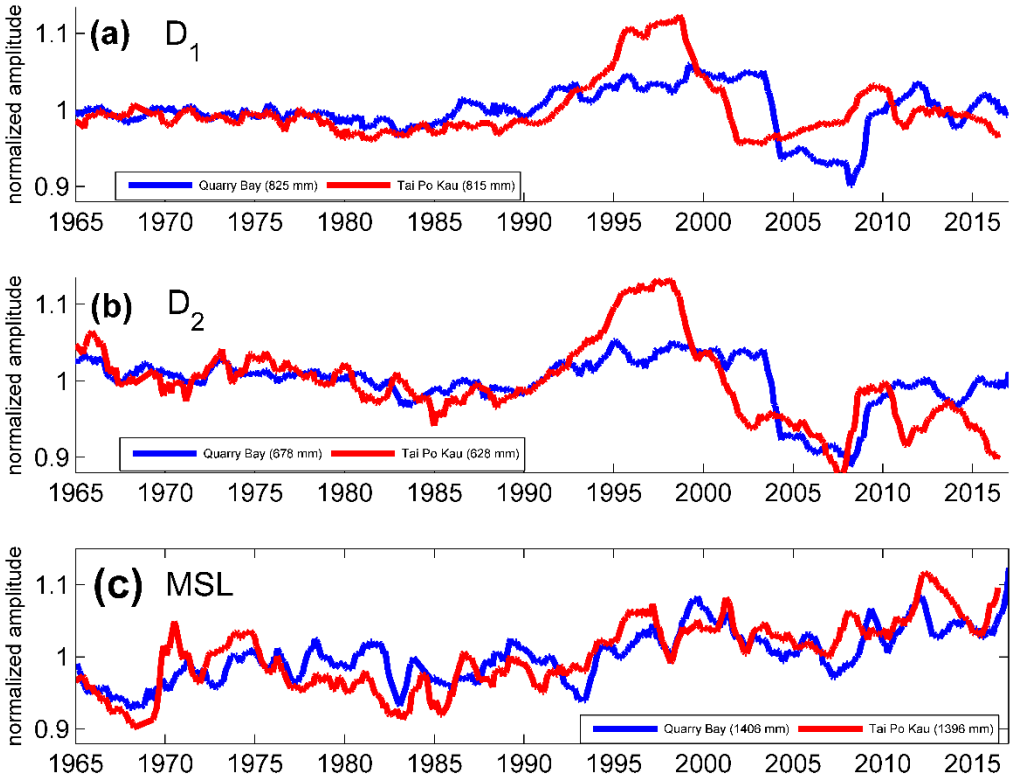

569

570 **Figure 9** Time series of water level spectrum components at the Quarry Bay (QB; blue) and
571 Tai Po Kau (TPK; red) tide gauges in Hong Kong, showing the D_1 band (a), the D_2 band (b),
572 and mean sea level (MSL) (c). Components are plotted as a function of normalized
573 amplitudes to show relative variability, with mean values given in the legend.

574

575

576

577

578

579

580

581

582

583 **REFERENCES:**

584 Alford, M. H.: Observations of parametric subharmonic instability of the diurnal internal tide
585 in the South China Sea. *Geophysical Research Letters*, 35, L15602, 2008.
586 doi:10.1029/2008GL034720

587 Amin, M.: On perturbations of harmonic constants in the Thames Estuary. Geophysical
588 Journal of the Royal Astronomical Society. *73*(3): 587-603. doi:10.1111/j.1365-
589 246X.1983.tb03334.x, 1983.

590 Arbic, B.K., Karsten, R.H., Garrett, C.: On tidal resonance in the global ocean and the back-
591 effect of coastal tides upon open-ocean tides. *Atmosphere-Ocean 47*(4), 239–266.
592 doi:10.3137/OC311.2009, 2009.

593 Arns, A., Dangendorf, S., Jensen, J., Bender, J., Talke, S.A., & Pattiaratchi, C.: Sea level rise
594 induced amplification of coastal protection design heights. *Nature: Scientific Reports,7*,
595 40171. doi:10.1038/srep40171, 2017.

596 Bowen, A. J., & Gray, D. A.: The tidal regime of the River Thames; long-term trends and
597 their possible causes. *Phil. Trans. R. Soc. Lond. A, 272*(1221), 187-199.
598 doi:10.1098/rsta.1972.0045, 1972.

599 Buchanan, M. K., Oppenheimer, M., & Kopp, R. E.: Amplification of flood frequencies with
600 local sea level rise and emerging flood regimes. *Environmental Research Letters, 12*(6),
601 064009. doi:10.1088/1748-9326/aa6cb3, 2017.

Cartwright, D.E., & Tayler, R.J.: New computations of the tide-generating potential. *Geophys. Journal of the Royal Astronomical Society*, *23*, 45-74. doi: 10.1111/j.1365-246X.1971.tb01803.x, 1971.

Cartwright, D.E.: Secular changes in the oceanic tides at Brest, 1711–1936. *Geophysical Journal International*, 30(4), 433-449. doi:10.1.1.867.2468, 1972.

Chernetsky, A. S., Schuttelaars, H. M., & Talke, S. A.: The effect of tidal asymmetry and temporal settling lag on sediment trapping in tidal estuaries. *Ocean Dynamics*, *60*(5), 1219-1241.. doi: 10.1007/s10236-010-0329-8, 2010.

Cherqui, F., Belmeziti, A., Granger, D., Sourdril, A., & Le Gauffre, P.: Assessing urban potential flooding risk and identifying effective risk-reduction measures. *Science of the Total Environment*, *514*, 418-425, 2015.

Chinn, B. S., Girton, J. B., & Alford, M. H.: Observations of internal waves and parametric subharmonic instability in the Philippines archipelago. *Journal of Geophysical Research: Oceans*, *117*(C5). doi:10.1029/2011JC007392, 2012.

Church, J. A., & White, N. J.: A 20th century acceleration in global sea-level rise. *Geophysical research letters*, *33*(1). doi:10.1029/2005GL024826, 2006.

Church, J. A., & White, N. J.: Sea level rise from the late 19th to the early 21st century. *Surveys in geophysics*, *32*(4-5), 585-602. doi 10.1007/s10712-011-9119-1, 2011.

Colosi, J. A., & Munk, W.: Tales of the venerable Honolulu tide gauge. *Journal of physical oceanography*, *36*(6), 967-996. doi:10.1175/JPO2876.1, 2006.

Craik, A.D.D.: Wave Interactions and Fluid Flows. Cambridge Univ. Press, Cambridge, U. K, ISBN: 978-0521368292, 1985.

Devlin, A. T., Jay, D. A., Talke, S. A., & Zaron, E.: Can tidal perturbations associated with sea level variations in the western Pacific Ocean be used to understand future effects of tidal evolution? *Ocean Dynamics*, *64*(8), 1093-1120. doi:10.1007/s10236-014-0741-6, 2014.

Devlin, A. T., Jay, D. A., Zaron, E. D., Talke, S. A., Pan, J., & Lin, H.: Tidal variability related to sea level variability in the Pacific Ocean. *Journal of Geophysical Research: Oceans*, *122*(11), 8445-8463. doi:10.1002/2017JC013165, 2017.

630 Devlin, A. T., Jay, D. A., Talke, S. A., Zaron, E. D., Pan, J., & Lin, H.: Coupling of sea level
631 and tidal range changes, with implications for future water levels. *Scientific Reports*, *7*(1),
632 17021. doi:10.1038/s41598-017-17056-z, 2017.

633 Devlin, A. T., Zaron, E. D., Jay, D. A., Talke, S. A., & Pan, J.: Seasonality of Tides in
634 Southeast Asian Waters. *Journal of Physical Oceanography*. doi: 10.1175/JPO-D-17-0119.1,
635 2018.

636 Devlin, A. T., Pan, J., & Lin, H.: Extended spectral analysis of tidal variability in the North
637 Atlantic Ocean. Journal of Geophysical Research: Oceans, 124(1), 506-526, 2019.

638 Domingues, C. M., Church, J. A., White, N. J., Gleckler, P. J., Wijffels, S. E., Barker, P. M.,
639 & Dunn, J. R.: Improved estimates of upper-ocean warming and multi-decadal sea level
640 rise. *Nature*, *453*(7198), 1090. doi:10.1038/nature07080, 2008.

641 Haigh, I. D., Wijeratne, E. M. S., MacPherson, L. R., Pattiaratchi, C. B., Mason, M. S.,
642 Crompton, R. P., & George, S.: Estimating present day extreme water level exceedance
643 probabilities around the coastline of Australia: tides, extra-tropical storm surges and mean sea
644 level. *Climate Dynamics*, *42*(1-2), 121-138. doi: 10.1007/s00382-012-1652-1, 2014.

645 Familkhalili, R., & Talke, S. A.: The effect of channel deepening on tides and storm surge: A
646 case study of Wilmington, NC. *Geophysical Research Letters*, *43*(17), 9138-9147.
647 doi:10.1002/2016GL069494, 2016.

648 Fang, G., Kwok, Y. K., Yu, K., & Zhu, Y.: Numerical simulation of principal tidal
649 constituents in the South China Sea, Gulf of Tonkin and Gulf of Thailand. *Continental Shelf*
650 *Research*, *19*(7), 845-869. doi: 10.1016/S0278-4343(99)00002-3, 1999.

651 Feng, X., Tsimplis, M. N., & Woodworth, P. L.: Nodal variations and long-term changes in
652 the main tides on the coasts of China. *Journal of Geophysical Research: Oceans*, *120*(2),
653 1215-1232. doi:10.1002/2014JC010312, 2015.

654 Ip, S.F. and Wai, H.G.: *An application of harmonic method to tidal analysis and prediction in*
655 *Hong Kong*. Royal Observatory, 1990.

656 Jan, S., Chern, C. S., Wang, J., & Chao, S. Y.: Generation of diurnal K_1 internal tide in the
657 Luzon Strait and its influence on surface tide in the South China Sea. *Journal of Geophysical*
658 *Research: Oceans*, *112*(C6). doi:10.1029/2006JC004003, 2007.

659 Jan, S., Lien, R. C., & Ting, C. H.: Numerical study of baroclinic tides in Luzon
660 Strait. *Journal of Oceanography*, *64*(5), 789. doi:10.1007/s10872-008-0066-5, 2008.

Jay, D. A. (2009). Evolution of tidal amplitudes in the eastern Pacific Ocean. *Geophysical Research Letters*, *36*(4). doi: 10.1029/2008GL036185

Leffler, K. E., & Jay, D. A.: Enhancing tidal harmonic analysis: Robust (hybrid L1/L2) solutions. *Continental Shelf Research*, *29*(1), 78-88. doi: 10.1016/j.csr.2008.04.011, 2009.

Li, K. W., & Mok, H. Y.: Long term trends of the regional sea level changes in Hong Kong and the adjacent waters. In *Asian And Pacific Coasts 2011* (pp. 349-359). doi:10.1142/9789814366489_0040, 2012.

Lien, R. C., Tang, T. Y., Chang, M. H., & d'Asaro, E. A.: Energy of nonlinear internal waves in the South China Sea. *Geophysical Research Letters*, *32*(5). doi:10.1029/2004GL022012, 2005.

MacKinnon, J. A., & Winters, K. B.: Subtropical catastrophe: Significant loss of low-mode tidal energy at 28.9°. *Geophysical Research Letters*, *32*(15). doi:10.1029/2005GL023376, 2005.

Mawdsley, R. J., Haigh, I. D., & Wells, N. C.: Global changes in mean tidal high water, low water and range. *Journal of Coastal Research*, *70*(sp1), 343-348. doi:10.2112/SI70-058.1, 2014.

McComas, C. H., & Bretherton, F. P.: Resonant interaction of oceanic internal waves. *Journal of Geophysical Research*, *82*(9), 1397-1412. doi:10.1029/JC082i009p01397, 1977.

Moftakhari, H. R., AghaKouchak, A., Sanders, B. F., Feldman, D. L., Sweet, W., Matthew, R. A., & Luke, A.: Increased nuisance flooding along the coasts of the United States due to sea level rise: Past and future. *Geophysical Research Letters*, *42*(22), 9846-9852. doi:10.1002/2015GL066072, 2015.

Moftakhari, H. R., AghaKouchak, A., Sanders, B. F., & Matthew, R. A.: Cumulative hazard: The case of nuisance flooding. *Earth's Future*, *5*(2), 214-223. doi:10.1002/2016EF000494, 2017.

Müller, M., Arbic, B. K., & Mitrovica, J. X.: Secular trends in ocean tides: Observations and model results. *Journal of Geophysical Research: Oceans*, *116*(C5) doi: 10.1029/2010JC006387, 2011.

Müller, M., Cherniawsky, J. Y., Foreman, M. G. G., & Storch, J. S.: Global M_2 internal tide and its seasonal variability from high resolution ocean circulation and tide modeling. *Geophysical Research Letters*, *39*(19). doi:10.1029/2012GL053320, 2012.

Müller, M.: The influence of changing stratification conditions on barotropic tidal transport and its implications for seasonal and secular changes of tides. *Continental Shelf Research, 47*, 107-118. doi: 10.1016/j.csr.2012.07.003, 2012.

Pan, J., Gu, Y. and Wang, D.: Observations and numerical modeling of the Pearl River plume in summer season, *Journal of Geophysical Research*, 119, doi:10.1002/2013JC009042, 2014.

Pawlowicz, R., Beardsley, B., & Lentz, S.: Classical tidal harmonic analysis including error estimates in MATLAB using T_TIDE. *Computers & Geosciences*, *28*(8), 929-937. doi:10.1016/S0098-3004(02)00013-4, 2002.

Rasheed, A. S., & Chua, V. P.: Secular trends in tidal parameters along the coast of Japan. *Atmosphere-Ocean, 52*(2), 155-168. doi:10.1080/07055900.2014.886031, 2014.

Ray, R. D.: Secular changes of the M_2 tide in the Gulf of Maine. *Continental shelf research, 26*(3), 422-427. doi: 10.1016/j.csr.2005.12.005, 2006.

Ray, R. D., & Foster, G.: Future nuisance flooding at Boston caused by astronomical tides alone. *Earth's Future*, *4*(12), 578-587. doi:10.1002/2016EF000423, 2016.

Ross, A. C., Najjar, R. G., Li, M., Lee, S. B., Zhang, F., & Liu, W.: Fingerprints of Sea Level Rise on Changing Tides in the Chesapeake and Delaware Bays. *Journal of Geophysical Research: Oceans*, *122*(10), 8102-8125. doi:10.1002/2017JC012887, 2017.

Sweet, W. V., & Park, J.: From the extreme to the mean: Acceleration and tipping points of coastal inundation from sea level rise. *Earth's Future*, 2(12), 579-600, 2014.

Vellinga, N. E., Hoitink, A. J. F., van der Vegt, M., Zhang, W., & Hoekstra, P.: Human impacts on tides overwhelm the effect of sea level rise on extreme water levels in the Rhine–Meuse delta. *Coastal Engineering*, *90*, 40-50. doi: 10.1016/j.coastaleng.2014.04.005, 2014.

Woodworth, P. L.: A survey of recent changes in the main components of the ocean tide. *Continental Shelf Research, 30*(15), 1680-1691. doi: 10.1016/j.csr.2010.07.002, 2010.

Xie, X. H., Chen, G. Y., Shang, X. D., & Fang, W. D.: Evolution of the semidiurnal (M2) internal tide on the continental slope of the northern South China Sea. *Geophysical Research Letters*, *35*(13). doi:10.1029/2008GL034179, 2008.

Xie, X. H., Shang, X. D., van Haren, H., Chen, G. Y., & Zhang, Y. Z.: Observations of parametric subharmonic instability-induced near-inertial waves equatorward of the critical diurnal latitude. *Geophysical Research Letters*, *38*(5). doi:10.1029/2010GL046521, 2011.

Xie, X., Shang, X., Haren, H., & Chen, G.: Observations of enhanced nonlinear instability in the surface reflection of internal tides. *Geophysical Research Letters*, *40*(8), 1580-1586. doi:10.1002/grl.50322, 2013.

Zaron, E. D., & Jay, D. A.: An analysis of secular change in tides at open-ocean sites in the Pacific. *Journal of Physical Oceanography*, *44*(7), 1704-1726. doi:10.1175/JPO-D-13-0266.1, 2014.

Zhang, H., Wang, T., Liu, M., Jia, M., Lin, H., Chu, L. M., & Devlin, A. T.: Potential of Combining Optical and Dual Polarimetric SAR Data for Improving Mangrove Species Discrimination Using Rotation Forest. *Remote Sensing*, *10*(3), 467. doi: 10.3390/rs10030467, 2018.

TABLES:

Table 1 Metadata for all tide gauge locations, giving the station names and station codes, latitude/longitude, year of the available records, as well as the range of data analyzed.

Station	*Latitude*	*Longitude*	*Start Year*	*End Year*	*Number of years used*
Quarry Bay (QB)	22.27° N	114.21° E	1954	2016	31 (1986-2016)
Tai Po Kau (TPK)	22.42° N	114.19° E	1963	2016	31 (1986-2016)
Tsim Bei Tusi (TBT)	22.48° N	114.02° E	1974	2016	31 (1986-2016)
Chi Ma Wan (CMW)	22.22° N	114.00° E	1963	1997	36 (1963-1997)
Cheung Chau (CHC)	22.19° N	114.03° E	2004	2016	12 (2004-2016)
Lok On Pai (LOP)	22.35° N	114.00° E	1981	1999	18 (1981-1999)
Ma Wan (MW)	22.35° N	114.06° E	2004	2016	12 (2004-2016)
Tai Miu Wan (TMW)	22.26° N	114.29° E	1996	2016	20 (1996-2016)
Shek Pik (SP)	22.21° N	113.89° E	1999	2016	17 (1999-2016)
Waglan Island (WAG)	22.17° N	114.30° E	1995	2016	21 (1995-2016)
Ko Lau Wan (KLW)	22.45° N	114.34° E	2004	2016	12 (2004-2016)
Kwai Chung (KC)	22.31° N	114.12° E	2004	2016	12 (2004-2016)

Table 2 Amplitude TACs for M_2, S_2, K_1, and O_1 for the period of 1986-2016. All values given are in units of millimeter change in tidal amplitude for a 1-meter fluctuation in sea level (mm m^{-1}). Statistically significant positive values are given in bold italic text.

Station	**M_2 TAC**	**S_2 TAC**	**K_1 TAC**	**O_1 TAC**
Quarry Bay (QB)	***+218 ± 37***	***+85 ± 16***	***+220 ± 15***	***+146 ± 11***
Tai Po Kau (TPK)	***+267 ± 42***	***+98 ± 17***	***+190 ± 68***	***+100 ± 25***
Tsim Bei Tusi (TBT)	+7 ± 80	-10 ± 15	+32 ± 22	+24 ± 22
Chi Ma Wan (CMW)	***-58 ± 11***	-7 ± 5	-18 ± 8	***-37 ± 10***
Cheung Chau (CHC)	***-63 ± 20***	-22 ± 35	***+69 ± 48***	+50 ± 92
Lok On Pai (LOP)	***-81 ± 24***	-18 ± 8	+8 ± 32	-24 ± 12
Ma Wan (MW)	***-68 ± 4***	+1 ± 25	***+52 ± 4***	***-62 ± 21***
Tai Miu Wan (TMW)	+22 ± 59	-1 ± 9	+10 ± 22	+3 ± 8
Shek Pik (SP)	***+62 ± 29***	+11 ± 18	***+70 ± 4***	+28 ± 17
Waglan Island (WAG)	+1 ± 21	+3 ± 6	+9 ± 7	-9 ± 8
Ko Lau Wan (KLW)	-46 ± 39	-11 ± 17	+29 ± 65	+60 ± 57
Kwai Chung (KC)	-90 ± 46	-10 ± 29	-91 ± 226	***-202 ± 161***

Table 3 The δ-HAT and D_1/D_2 TACs for the period of 1986-2016. The δ-HAT values given are in units of millimeter change in tidal amplitude for a 1-meter fluctuation in sea level (mm m^{-1}). D_1/D_2 TACs are in unitless ratios (i.e., mm mm^{-1}) Statistically significant values are given in bold italic text.

Station	**δ-HAT**	**D_1/D_2**
Quarry Bay (QB)	***+665 ± 82***	***+1.08 ± 0.05***
Tai Po Kau (TPK)	***+612 ± 210***	***+1.01 ± 0.04***
Tsim Bei Tusi (TBT)	+56 ± 117	***+0.37 ± 0.02***
Chi Ma Wan (CMW)	***-119 ± 19***	***+0.74 ± 0.19***
Cheung Chau (CHC)	-12 ± 42	+0.81 ± 1.03
Lok On Pai (LOP)	-114 ± 45	***+0.26 ± 0.05***
Ma Wan (MW)	***-91*** ± ***73***	+0.57 ± 1.02
Tai Miu Wan (TMW)	+42 ± 100	***+1.04 ± 0.20***
Shek Pik (SP)	***+138*** ± ***37***	***+0.89 ± 0.06***
Waglan Island (WAG)	+3 ± 31	***+1.11 ± 0.17***
Ko Lau Wan (KLW)	-66 ± 47	***+1.31 ± 0.62***